"New" hepatic fat activates PPARα to maintain glucose, lipid, and cholesterol homeostasis

Manu V. Chakravarthy,[1,3] Zhijun Pan,[1,3] Yimin Zhu,[1] Karen Tordjman,[1] Jochen G. Schneider,[1] Trey Coleman,[1] John Turk,[1] and Clay F. Semenkovich[1,2,*]

[1]Endocrinology, Metabolism, and Lipid Research, Department of Medicine, Washington University School of Medicine, Campus Box 8127, 660 South Euclid Avenue, St. Louis, Missouri 63110
[2]Department of Cell Biology and Physiology, Washington University School of Medicine, St. Louis, Missouri 63110
[3]These authors contributed equally to this work.
*Correspondence: csemenko@im.wustl.edu

Summary

De novo lipogenesis is an energy-expensive process whose role in adult mammals is poorly understood. We generated mice with liver-specific inactivation of fatty-acid synthase (FAS), a key lipogenic enzyme. On a zero-fat diet, FASKOL (*FAS knockout in liver*) mice developed hypoglycemia and fatty liver, which were reversed with dietary fat. These phenotypes were also observed after prolonged fasting, similarly to fasted PPARα-deficiency mice. Hypoglycemia, fatty liver, and defects in expression of PPARα target genes in FASKOL mice were corrected with a PPARα agonist. On either zero-fat or chow diet, FASKOL mice had low serum and hepatic cholesterol levels with elevated *SREBP-2*, decreased *HMG-CoA reductase* expression, and decreased cholesterol biosynthesis; these were also corrected with a PPARα agonist. These results suggest that products of the FAS reaction regulate glucose, lipid, and cholesterol metabolism by serving as endogenous activators of distinct physiological pools of PPARα in adult liver.

Introduction

Primitive organisms exquisitely adapt gene expression to changes in nutrients that are frequently accessible across a single biological membrane. Complex organisms must balance metabolic supply and demand through physiological systems ensuring appropriate provision of substrates to tissues without direct access to a nutrient source. In mammals, the liver integrates nutrient intake and the delivery of carbohydrates and lipids to peripheral tissues. Hepatocytes, exposed to dietary signals (from portal blood flow) and systemic signals (from the arterial blood supply), coordinate gene expression and maintain homeostasis (Jump and Clarke, 1999; Langhans 2003). Abnormal hepatocyte function is central to common human diseases including type 2 diabetes (characterized by excessive hepatic glucose production), atherosclerosis (associated with excessive production of atherogenic lipoproteins by the liver), and steatohepatitis or fatty liver (commonly seen in obesity and insulin resistance).

Hepatocytes assimilate carbohydrate and lipid signals in part through PPARα, a member of the nuclear receptor superfamily (Berger and Moller, 2002). PPARs first appeared about 280 million years ago at the fish/mammal divergence (Latruffe and Vamecq, 2000), providing a molecular mediator for adapting to intermittent nutritional deprivation. PPARα stimulates the transcription of genes critical for fatty-acid oxidation (Reddy, 2001) and ketogenesis (Rodriguez et al., 1994). It also promotes gluconeogenesis through several mechanisms (Bernal-Mizrachi et al., 2003; Koo et al., 2004), including the stimulation of hepatic glycerol utilization (Patsouris et al., 2004). Highlighting the importance of PPARα in managing energy stores, PPARα-deficient mice develop hypoglycemia, hypoketonemia, and fatty

liver when subjected to a prolonged fast (Kersten et al., 1999). Fatty acids are thought to be the natural ligands for PPARα, but the precise origin of these activators is unknown.

SREBPs (sterol regulatory element binding proteins) are another class of proteins used by hepatocytes to coordinate carbohydrate and lipid metabolism (Horton et al., 2002). They reside in the ER and must be proteolytically cleaved in the Golgi to yield forms that are transcriptionally active. There are two predominant forms of SREBPs in animals, SREBP-1c, which stimulates fatty-acid synthesis, and SREBP-2, which stimulates cholesterol synthesis. Both are regulated by feeding/fasting. In particular, SREBP-1c participates in de novo lipogenesis when dietary carbohydrates are abundant. *SREBP-1c* transcription is affected by circulating levels of insulin and glucagon, critical hormones in glucose homeostasis, and the oxysterol receptor LXR (Chen et al., 2004). *SREBP-2* transcription is affected by cholesterol availability. Fatty acids can affect *SREBP* expression (Xu et al., 2002a; Pawar et al., 2003).

Hepatic fatty acids for activating PPARα and altering *SREBP* expression can be derived from several sources. One simple way to discriminate between sources is by classifying fat as "new" or "old." Fatty acids synthesized from carbohydrates represent new fat. Dietary fatty acids transported to the liver in chylomicrons represent another source of new fat. New fat might be retained in the liver (for storage, energy production, or the synthesis of structural and signaling lipids) or exported in VLDL to peripheral tissues for metabolism or storage. In the appropriate milieu, stored or old fat is released from adipose tissue into the circulation. Those fatty acids not utilized for energy are returned to the liver where the ultimate fate of this old fat is poorly understood. Whether new and old fatty acids are interchangeable or if fatty acids from certain sources are channeled to specific functions is unknown.

To test the hypothesis that the metabolic fate of fatty acids depends on their site of origin, we engineered mice with liver-specific inactivation of fatty-acid synthase, the enzyme catalyzing the first committed step in fatty-acid biosynthesis (Semenkovich, 1997). FAS is a large multifunctional protein with seven catalytic domains required to convert dietary carbohydrates into saturated fatty acids, mostly palmitate (C16:0). Germline FAS$^{-/-}$ mice die at the preimplantation stage, and even FAS$^{+/-}$ mice have increased fetal demise, indicating an absolute requirement for FAS function during embryonic development (Chirala et al., 2003). Unlike FAS$^{-/-}$ mice, FASKOL (for *FAS knockout in liver*) animals are viable, allowing us to assess the impact of hepatic de novo lipogenesis on metabolism. Our results show that new but not old fat activates physiologically distinct pools of PPARα in liver to affect glucose, fatty-acid, and cholesterol homeostasis.

Results

Generation of FASKOL mice
ES cells, identified as appropriately targeted by a vector with loxP sites flanking exons 4–8 of the mouse *FAS* gene (Figure 1A), were used to generate chimeric mice. Animals carrying the targeted allele transmitted this locus through the germline to yield mice heterozygous for the targeted allele (lox$^+$/wt [wild-type]). Intercrossing lox$^+$/wt mice yielded offspring consistent with Mendelian inheritance (24% lox$^+$/lox$^+$, 22% wt/wt, and 54% lox$^+$/wt). All three genotypes were indistinguishable in terms of body weight, body composition, hepatic *FAS* mRNA, hepatic FAS enzyme activity, and plasma chemistries (data not shown), indicating that the loxP sites and NEO cassette did not interfere with *FAS* expression.

Mice carrying the "silent" targeted allele were crossed with animals expressing *Cre* recombinase driven by the adenovirus EIIa promoter (EIIaCre). EIIaCre-mediated recombination occurs early in development (2–8 cell stage) and at low levels, resulting in chimerism with selective deletion of the NEO cassette in some animals. Analysis of DNA from offspring of lox$^+$/wt × EIIaCre$^{+/-}$ matings documented the presence of all possible deletion patterns. As expected, intercrossing mice carrying the floxed allele with the NEO cassette deleted yielded Mendelian proportions of each genotype, normal body and plasma characteristics, and normal hepatic *FAS* mRNA as well as enzyme activity in each genotype (data not shown). The lox$^+$/wt × EIIaCre cross also produced FAS-deficient alleles (heterozygotes with deletions of exons 4–8). FAS enzyme activity was decreased by ∼50% in tissues of heterozygotes, and multiple intercrosses using these mice produced no homozygotes, confirming the embryonic lethality of complete FAS deficiency (Chirala et al., 2003).

FASKOL mice, with liver-specific inactivation of the *FAS* gene, were produced by crossing lox$^+$/wt mice with rat albumin promoter-Cre transgenic mice, which express Cre exclusively in postpartum liver (Postic and Magnuson, 2000). Double heterozygous [lox$^+$/wt Cre$^{+/-}$] progeny were mated with lox$^+$/wt littermates (lacking the albumin-Cre transgene) to yield FASKOL mice [lox$^{+/+}$ Cre$^+$] as well as three different groups of littermate controls: [lox$^{+/+}$ Cre$^-$], [lox$^{-/-}$ Cre$^+$], and [lox$^{-/-}$ Cre$^-$]. FASKOL mice were born at the expected frequency of 12.5%, indicating that the combination of the floxed allele and the Cre transgene was not associated with prenatal lethality. Newborn FASKOL

mice were indistinguishable from their control littermates, nursed successfully, weaned normally, and were active and fertile.

Rearrangement of the *FAS* gene was restricted to the liver in FASKOL mice (Figure 1B). Southern blotting revealed a 7.3 kb native allele in DNA from control mice (W in Figure 1B) carrying the *Cre* transgene without the floxed *FAS* gene. Only the 8.9 kb floxed allele was detected in nonhepatocyte DNA from FASKOL (F in Figure 1B) mice. A 5.3 kb fragment, the predicted size following deletion of exons 4–8, was detected only in FASKOL (F) liver but not lung, heart, brain, kidney, or skeletal muscle. It was also absent from liver of mice carrying the floxed allele without Cre (F$^-$ in Figure 1B). A less intense band at 8.9 kb, representing the floxed allele without rearrangement, was also present in DNA from FASKOL liver, reflecting nonhepatocytes in liver that would not be expected to transactivate the albumin promoter to express Cre. Liver-specific rearrangement of the *FAS* gene in FASKOL mice was confirmed by PCR. A 317 bp product indicating deletion of exons 4–8 was seen only in liver in the presence of the floxed locus and Cre (Figure 1C, lane 3), not in livers of three different control mice (lanes 2,4,5), and not in other FASKOL tissues such as heart (lane 7).

Liver FAS enzyme activity was decreased by ∼80% (range 65%–95%) in FASKOL mice as compared to animals from three different control groups (Figure 1D, upper panel). Maximal effects were not seen until the age of 16–20 weeks. Since FAS expression is ubiquitous and hepatocytes comprise 80%–85% of liver cells, residual liver activity in FASKOL mice is likely due to nonparenchymal cells. FAS activity was unaffected in lung (inset, Figure 1D), adipose tissue, heart, and brain of FASKOL mice.

Since FAS synthesizes palmitate (C16:0) from malonyl-CoA, inactivation of FAS should increase malonyl-CoA and decrease palmitate. In overnight-fasted-12 hr chow-refed mice (Figure 1D, lower panel), malonyl-CoA content was 3-fold higher (14.1 ± 3 nmol/g tissue) in FASKOL liver as compared to animals carrying the floxed allele without Cre (4.5 ± 2.3 nmol/g tissue). Levels were unaffected in other tissues of FASKOL mice (not shown). To evaluate metabolism under conditions known to be associated with induction of FAS activity, mice were fed a high-carbohydrate diet without fat (zero-fat diet or ZFD). The difference in hepatic malonyl-CoA persisted under these conditions: 11.0 ± 2.1 nmol/g in FASKOL versus 5.1 ± 1.6 nmol/g in controls. Without a dietary source of palmitate (ZFD), hepatic palmitate content assayed by GC/MS using deuterated palmitic acid as internal standard was decreased in FASKOL mice (Figure 1E) as compared to control mice ("wt" or lox$^{+/+}$ Cre$^-$)

Metabolic characterization of FASKOL mice
Although there were no phenotypic differences among the three different control mouse groups, all subsequent comparisons were made between FASKOL mice and lox$^{+/+}$ Cre$^-$ (wt) mice. On a normal chow diet, FASKOL mice had lower fasting insulin levels and a lower insulin/glucagon ratio compared to wt mice, but there were no differences in body weight, adiposity, metabolic rate, food intake, and several other metabolic parameters (Table 1). Serum cholesterol was the notable exception; fasting cholesterol was ∼40% lower (p < 0.01) in chow-fed FASKOL mice (see below).

The effects of the ZFD in FASKOL mice were striking. Fasting glucose decreased 50%–60% in FASKOL mice, insulin levels
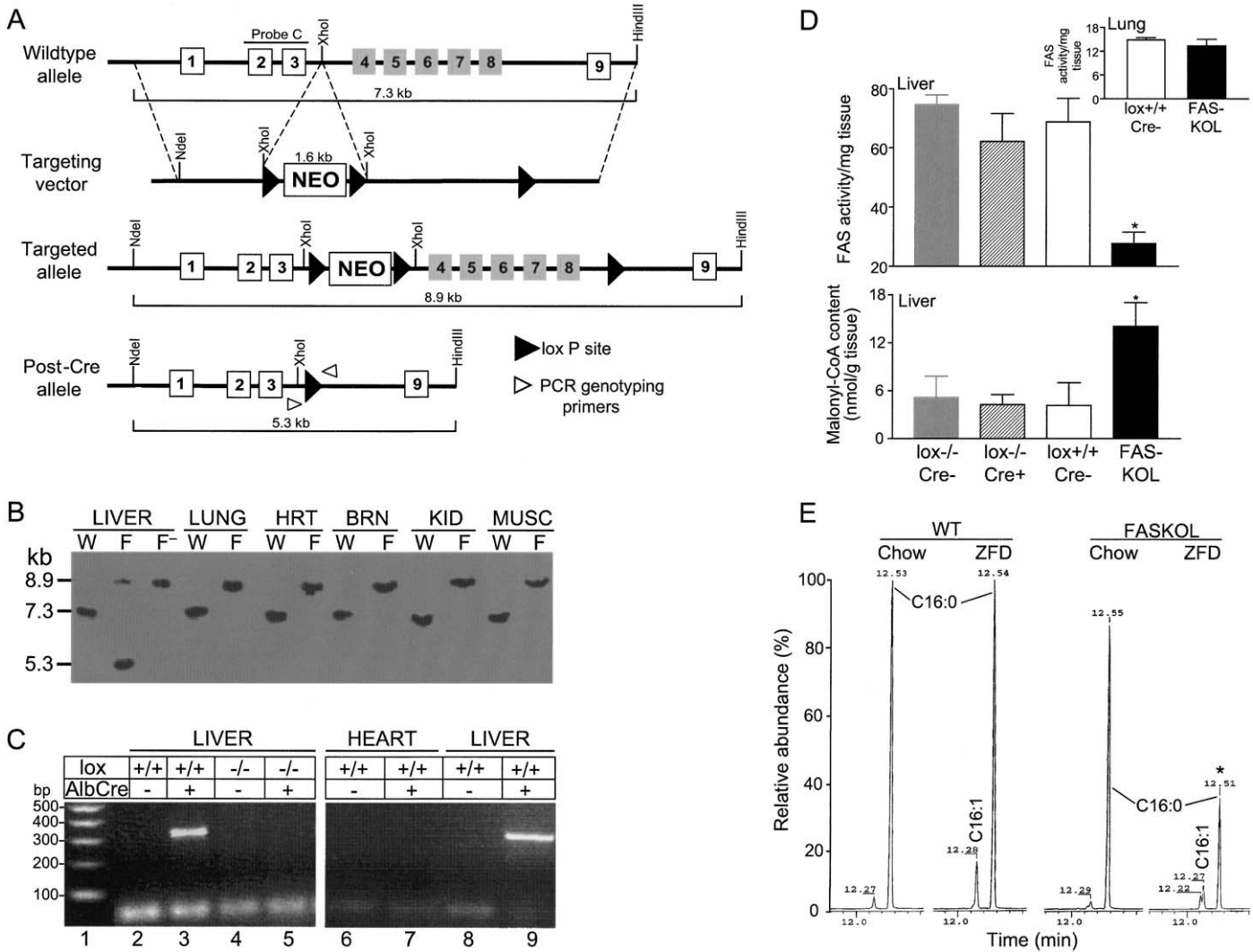
Figure 1. Targeting of the fatty-acid synthase gene

A) Wild-type, targeting vector, and the fatty-acid synthase (FAS) lox allele before and after recombination. The post-Cre allele depicts the deletion of exons 4–8 (gray shaded boxes). NEO, neomycin positive-selection cassette; open boxes, exons preserved; black arrowheads, loxP sites; open arrowheads, genotyping primers.

B) Southern blot analysis of DNA from control (W, $lox^{-/-}$ Cre^+; F^-, $lox^{+/+}$ Cre^-) and FASKOL (F, $lox^{+/+}$ Cre^+) mice. Genomic DNA (from liver, lung, heart, brain, kidney, and skeletal muscle) was digested with NdeI and HindIII and detected using probe C to yield the expected fragments of 7.3 kb (allele without loxP), 8.9 kb (floxed allele), and 5.3 kb (post-Cre allele).

C) PCR analysis. DNA from FASKOL livers ($lox^{+/+}$ Cre^+) produced a 317 bp product (lane 3) indicating appropriate deletion at the FAS gene. The product was absent in the livers of wt control mice of various genotypes. It was also absent in hearts of FASKOL mice (lane 7).

D) Assessment of FAS activity (upper panel) and malonyl-CoA content (lower panel). Liver homogenates from overnight-fasted 12 hr chow-refed male FASKOL (black bar) and littermate control mice of various genotypes aged 16–20 weeks were assayed for FAS enzyme activity and malonyl-CoA content. The inset of (**D**) represents FAS activity in lung tissue of FASKOL (black bar) and wt ($lox^{+/+}$ Cre^-, white bar) mice. Each bar represents the mean ± SEM of eight mice of each genotype. *, $p < 0.05$.

E) Gas chromatography retention peaks of hepatic palmitate (C16:0) and palmitoleate (C16:1) from chow and zero-fat diet (ZFD) fed wt ($lox^{+/+}$ Cre^-) and FASKOL mice. Data are representative of two independent experiments with four mice per group. The molecular identities of these retention peaks were verified and quantitated by mass spectrometry. *, $p < 0.05$.

remained low, but glucagon, the key hormonal defense against hypoglycemia in mammals, increased by ~50% (Table 1). Consistent with stimulation of lipolysis in peripheral tissues by glucagon, in ZFD-fed FASKOL mice, fat pad weight decreased, whole-body adiposity decreased, serum NEFA increased, and liver weight increased in the setting of a modest increase in the transaminase ALT without affecting other liver function tests (Table 1). Peripheral fat stores were depleted in ZFD-fed FASKOL mice, reflected by decreased leptin levels compared

to ZFD-fed wt mice, and the livers were obviously pale in ZFD-fed FASKOL mice (not shown), suggesting the presence of hepatic steatosis.

Reversal of hypoglycemia and fatty liver in FASKOL mice

ZFD-fed FASKOL mice had distinct, reversible alterations in hepatic morphology. After 28 days of ZFD, FASKOL mice were hypoglycemic (Figure 2A), liver triglyceride content was increased

Table 1. Comparisons of wt and FASKOL mice on chow and zero-fat diet

Parameters	Chow		ZFD	
	wt	FASKOL	wt	FASKOL
Metabolites and hormones				
Glucose (mg/dl)	161 ± 16	145 ± 11	169 ± 13	104 ± 12[a,b]
NEFA (mEq/l)	0.58 ± 0.04	0.54 ± 0.05	0.48 ± 0.03	0.76 ± 0.1[a,b]
Insulin (ng/ml)	1.34 ± 0.82	0.63 ± 0.05[a]	0.94 ± 0.09	0.54 ± 0.14[a]
Glucagon (pg/ml)	128.3 ± 16.2	134.7 ± 13.1	141.3 ± 12.4	200.0 ± 11.8[a,b]
Insulin/glucagon ratio	10.4 ± 0.98	4.7 ± 0.18[a]	6.7 ± 0.21	2.7 ± 0.26[a]
Leptin (pg/ml)	919.6 ± 162	881.6 ± 132	7712 ± 1149[b]	1701 ± 330[a,b]
Adiponectin (ng/ml)	7776 ± 452	7613 ± 312	9012 ± 501	9038 ± 1094
Liver function				
ALT (IU/l)	47.0 ± 11	32.0 ± 3.4	32.0 ± 5.3	52.0 ± 13.1[a,b]
Alk phosphatase (IU/l)	88 ± 1.4	91 ± 2.7	81 ± 1.6	94 ± 1.2
Total Bilirubin (mg/dL)	0.27 ± 0.04	0.31 ± 0.08	0.3 ± 0.06	0.33 ± 0.07
Albumin (g/dl)	2.8 ± 0.1	3.0 ± 0.2	3.1 ± 0.2	3.2 ± 0.14
Energy balance				
Body weight (g)	26.5 ± 1.5	26.4 ± 1.2	29.2 ± 2.0	28.4 ± 1.7
Fat content by DEXA (%)	15.5 ± 3.1	13.9 ± 2.0	17.3 ± 3.4	11.4 ± 2.6[a]
VO$_2$ (ml/g$^{0.75}$/h)	9.61 ± 1.23	9.2 ± 1.05	10.01 ± 2.04	9.80 ± 1.1
Liver/BW ratio	0.043 ± 0.002	0.039 ± 0.002	0.045 ± 0.003	0.061 ± 0.002[a,b]
Fat pad/BW ratio	0.026 ± 0.004	0.022 ± 0.004	0.023 ± 0.002	0.013 ± 0.003[a,b]
Food intake (g/day)	5.35 ± 0.26	5.55 ± 0.05	3.36 ± 0.16[b]	3.2 ± 0.41[b]

Male mice (16–20 weeks, n = 6 per group) were either maintained on chow or ZFD for 17 days. Animals were fasted for 4 hr prior to study. Each value represents the mean ± SEM of six values. p < 0.05 for the following: [a]compared to corresponding wt mice; [b]compared to the corresponding chow-fed mice. BW, body weight. DEXA, dual-energy x-ray absorptiometry.

(Figure 2B), and plasma ALT levels were modestly increased (Figure 2C). ZFD-induced hypoglycemia and ALT elevation in FASKOL mice resolved completely after reinstitution of chow diet for 17 days with values similar to those seen in control mice fed chow only. However, hepatic triglycerides remained elevated albeit at significantly lower levels than on ZFD (Figures 2A–2C). Hepatic glycogen stores, determined by PAS staining, were decreased in ZFD-fed FASKOL mice (Figure 2E, middle panel) compared to ZFD-fed wt mice (Figure 2D, middle panel) and replenished after reintroduction of chow (Figure 2E, lower panel). Hepatic lipid content, determined by oil red O staining (ORO), mirrored the quantitative hepatic triglyceride determination—increased in ZFD-fed FASKOL mice (Figure 2E, middle panel) compared to ZFD-fed wt mice (Figure 2D, middle panel) and significantly reduced after chow feeding (Figure 2E, lower panel). As controls, liver sections from chow-only fed wt and FASKOL mice were also stained with PAS and ORO (Figures 2D and 2E, upper panel), and they showed no difference between the genotypes.

Hypoglycemia and steatohepatitis are characteristic of PPARα deficiency. To determine if the metabolic derangements in ZFD-fed FASKOL mice were related to defective activation of PPARα-dependent pathways, the potent PPARα activator Wy14,643 was incorporated into both the chow and zero-fat diets. A time course of the effects of ZFD on fasting glucose is shown in Figure S1A. Glucose tended to be lower by 3 days and plateaued at significantly lower levels between days 10 and 28. Consumption of the Wy compound with ZFD for 10 days significantly increased glucose levels in FASKOL mice compared to FASKOL mice eating the ZFD alone (Figure 3A). In contrast, addition of the Wy compound to chow diet for 10 days did not result in a significant change in glucose in either wt or FASKOL mice compared to chow diet alone (Figure 3A). ZFD-induced hypoglycemia in FASKOL mice was associated with lower glucose levels at all time points in intraperitoneal (i.p.) glucose tolerance tests compared to ZFD-fed wt mice (Figure S1B, upper panel). Incorporation of the Wy compound into the ZFD tended to raise glucose levels in FASKOL mice relative to wt. However, there were no differences in insulin-tolerance tests between the genotypes with any of the dietary treatments (Figure S1B, lower panel). Thirty minutes after i.p. glucose, FASKOL mice showed decreased glucose with insulin levels similar to wt (Figure S1C). C peptide and insulin ratios were also similar between the genotypes on both chow and ZFD (Figure S1D).

The hormonal response to ZFD-induced hypoglycemia in FASKOL mice was appropriate, with decreased insulin (Figure 3B) and increased glucagon (Figure 3C), yielding a low insulin/glucagon ratio (Figure 3D) compared to normoglycemic ZFD-fed wt mice. The Wy compound fed with either chow or ZFD had no effect on insulin/glucagon ratios, although absolute insulin and glucagon levels were reduced in ZFD+Wy-fed wt and FASKOL mice (Figures 3B–3C).

Hepatic glycogen depletion and triglyceride accumulation in ZFD-fed FASKOL mice were also prevented by the Wy compound. Lower glycogen content in ZFD-fed FASKOL mice (8.6 ± 1.8 μmol/g) compared to ZFD-fed wt mice (17.8 ± 4.1 μmol/g) did not occur in ZFD+Wy-fed FASKOL mice nor in chow+ Wy-treated wt and FASKOL mice (Figure 3E). ZFD-fed FASKOL liver triglyceride content (14.1 ± 0.33 mg/g) was nearly twice that of ZFD-fed wt livers (8.3 ± 0.28 mg/g) but not in the presence of dietary Wy compound (Figure 3F). No further reduction in hepatic triglyceride content was noted in either wt or FASKOL mice treated with chow+Wy, compared to chow feeding alone. This quantitative analysis was confirmed histologically, as shown in Figures 3K and 3L. The marked steatosis noted in ZFD-fed FASKOL mice (Figure 3L, 2nd panel) did not occur in the presence of Wy compound (Figure 3L, 4th panel).
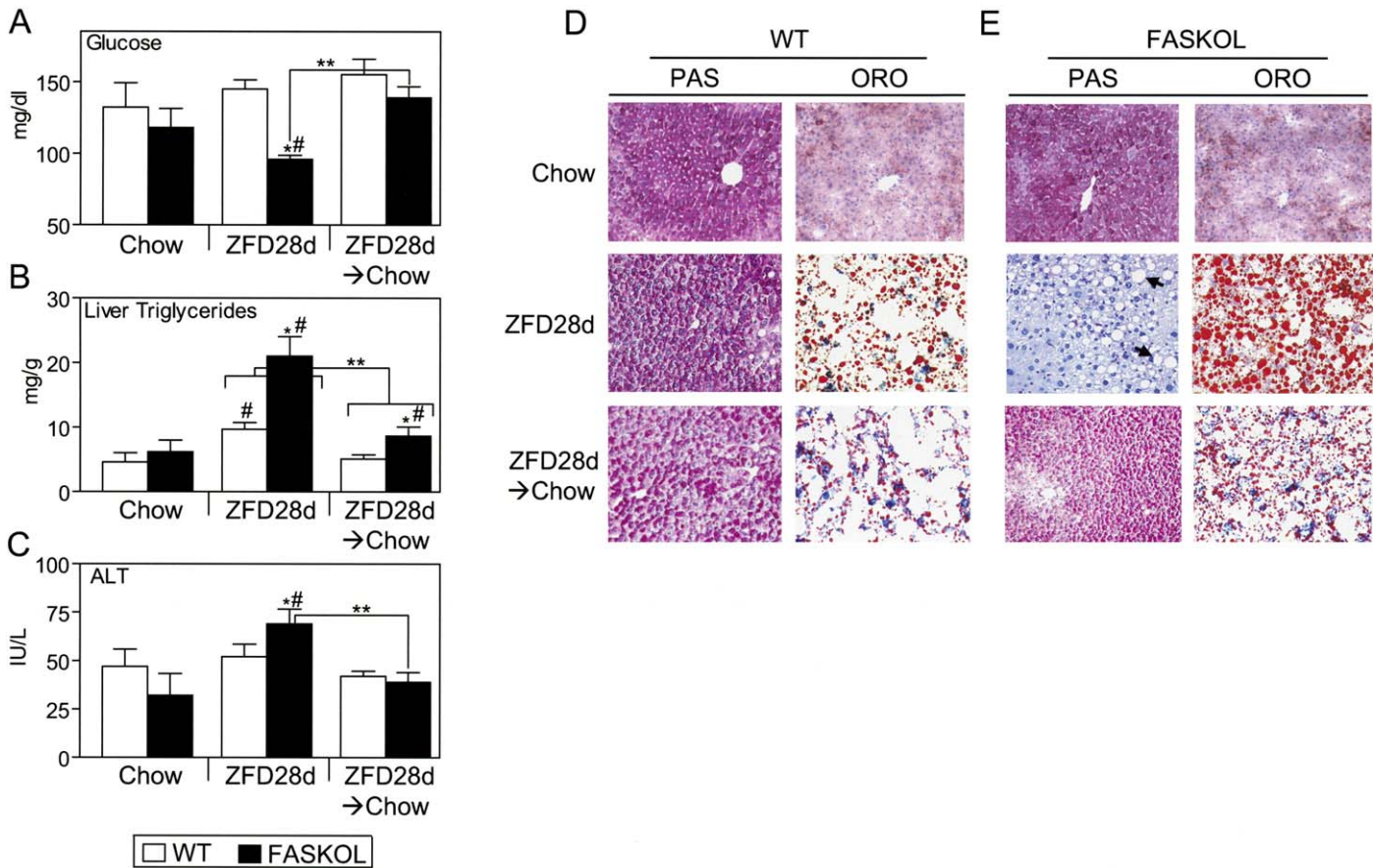
Figure 2. Zero-fat diet induces relative hypoglycemia with glycogen depletion and steatohepatitis that is reversed with chow feeding

A–C) Four hour fasting serum glucose (**A**), liver triglyceride (**B**), and alanine aminotransferase (**C**) concentrations in 16- to 20-week-old male wt (lox$^{+/+}$ Cre$^-$, white bars) and FASKOL (black bars) mice fed ZFD for 28 days (ZFD28d) and then switched to chow (ZFD28d→chow), or maintained only on chow for the duration of the study (Chow). Each bar represents the mean ± SEM of 4–5 mice of each genotype per group. $p < 0.05$ for the following: *, compared to the corresponding wt mice; #, compared to the corresponding chow-fed mice; **, compared to the corresponding 28 day ZFD-fed mice.

D and E) Liver histology for wt (lox$^{+/+}$ Cre$^-$) and FASKOL mice. After 28 days of ZFD feeding (middle panel), subgroups of the 16- to 20-week-old wt and FASKOL mice were switched to chow diet for 17 days (lower panel). As controls, four mice from each genotype were maintained only on chow diet for the duration of the study (upper panel). Sections from chow-only fed (chow), ZFD-fed (ZFD28d), and chow-switched (ZFD28d→chow) animals were stained with periodic acid schiff (PAS) or oil red O (ORO), magnification 10×. Vacuolation seen in 28 day ZFD-fed FASKOL mice (arrows) was mostly lipid as shown by ORO staining. Sections are representative of several animals for each condition.

Serum triglyceride and NEFA levels (Figures 3G and 3H) in both wt and FASKOL mice were markedly decreased upon ingestion of Wy in both chow and ZFD, as expected.

FASKOL mice on a chow diet had low levels of serum and hepatic cholesterol that were unaffected by ZFD feeding (Figures 3I and 3J). Both were increased in FASKOL mice when PPARα was activated using Wy14,643 in both the chow and ZFD (Figures 3I and 3J). In contrast, there were no significant effects on cholesterol levels in wt mice fed chow+Wy (Figures 3I and 3J).

The reversal of hypoglycemia and hypocholesterolemia after ZFD+Wy feeding in FASKOL mice suggested that activation of PPARα-dependent pathways was involved. To determine if PPARα deficiency contributed to the phenotype, whole-body PPARα knockout (PPARα$^{-/-}$) mice were subjected to the same dietary challenge described above. Despite having a lower fasting glucose on chow, PPARα$^{-/-}$ mice did not manifest any further decrease in glucose levels after 10 days of ZFD feeding (Figure

S2A). Glucose levels were unaffected by Wy feeding with either chow or ZFD. In contrast, C57BL/6 littermate control mice had significantly higher glucose on chow that decreased after ZFD+Wy feeding (Figure S2A). Similarly, cholesterol levels were unaffected in PPARα$^{-/-}$ mice regardless of diet and remained significantly higher than C57BL/6 control mice with both chow and ZFD feeding (Figure S2B). Consistent with previous reports (Xu et al., 2002b), fasting insulin levels in PPARα$^{-/-}$ mice tended to be higher than in the C57BL/6 control mice under all dietary conditions (not shown). Also as expected in the PPARα$^{-/-}$ mice, NEFA levels were higher than in control mice, with no decrease in either NEFA or triglyceride levels after Wy feeding, in contrast to control mice (Figures S2C and S2D).

PPARα activation and the expression of glucose metabolism genes

To address the mechanisms by which ZFD-fed FASKOL mice manifest hypoglycemia and their subsequent restoration to
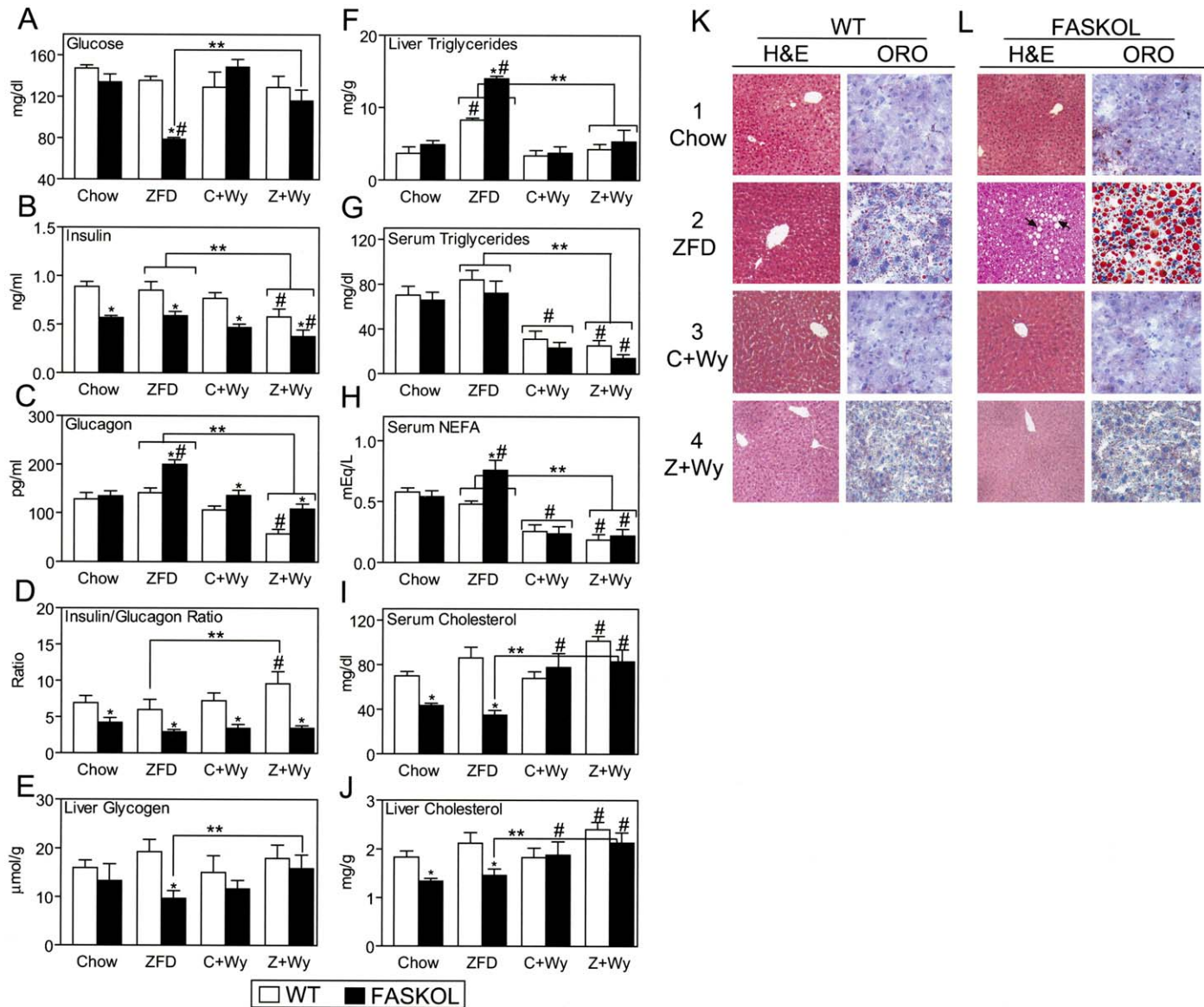
Figure 3. Effects of PPARα activation on glucose and lipid homeostasis in FASKOL and wt (lox^{+/+} Cre[−]) mice

A–J) Measurements of serum glucose (**A**), insulin (**B**), glucagon (**C**), insulin to glucagon ratio (**D**), liver glycogen (**E**), liver triglycerides (**F**), serum triglycerides (**G**), serum nonesterified fatty acids (**H**), serum total cholesterol (**I**), and liver cholesterol content (**J**) were obtained from 4 hr fasted wt and FASKOL mice on chow or zero-fat diet for 10 days (ZFD), or PPARα agonist Wy14,643 added to chow (C+Wy) or ZFD (Z+Wy) for 10 days. Each bar represents the mean ± SEM values of 6–8 male wt and FASKOL mice, aged 16–20 weeks, fed the various diets. p < 0.05 for the following: *, compared to the corresponding wt mice; #, compared to the corresponding chow-fed mice; **, compared to the corresponding ZFD-fed mice. White bars, wt; black bars, FASKOL.

K and L) Liver histology for chow (panel 1), ZFD for 10 days (panel 2), chow+Wy14,643 for 10 days (panel 3), and ZFD+Wy14,643 for 10 days (panel 4) fed wt and FASKOL mice. Liver sections from the above animals were stained with hematoxylin and eosin (H&E) and oil red O (ORO), magnification 10×. The prominent vacuolation seen in ZFD-fed FASKOL mice (arrows, panel 2) stained positive for ORO (panel 2). Sections are representative of several animals for each condition.

normoglycemia with PPARα activation, we studied the expression of PPARα target genes critical for gluconeogenesis (Figure 4). Messenger RNA levels for *PPARα* itself were unaffected in FASKOL mice on chow and ZFD in liver (Figure 4A), as well as in kidney and heart, two other tissues known to have high *PPARα* expression (Figure S3A). *PPARα* mRNA levels were appropriately induced after both chow+Wy and ZFD+Wy feeding in all tissues analyzed (Figure 4A and Figure S3A) since PPARα activation is known to stimulate its own transcription.

Induction of gluconeogenic genes is regulated in part through PGC-1α, via PPARα-dependent induction of *TRB3* (Koo et al., 2004). Expression of these genes was markedly changed in ZFD-fed FASKOL livers and responded to PPARα activation. *PGC-1α* expression was increased in ZFD-FASKOL livers (Figure 4A), likely due to elevated glucagon (Figure 3C), and appropriately stimulated by Wy in both genotypes on ZFD, but only in the FASKOL mice on chow+Wy (Figure 4A). Expression of *TRB3*, a recently identified PPARα target (Koo et al.,
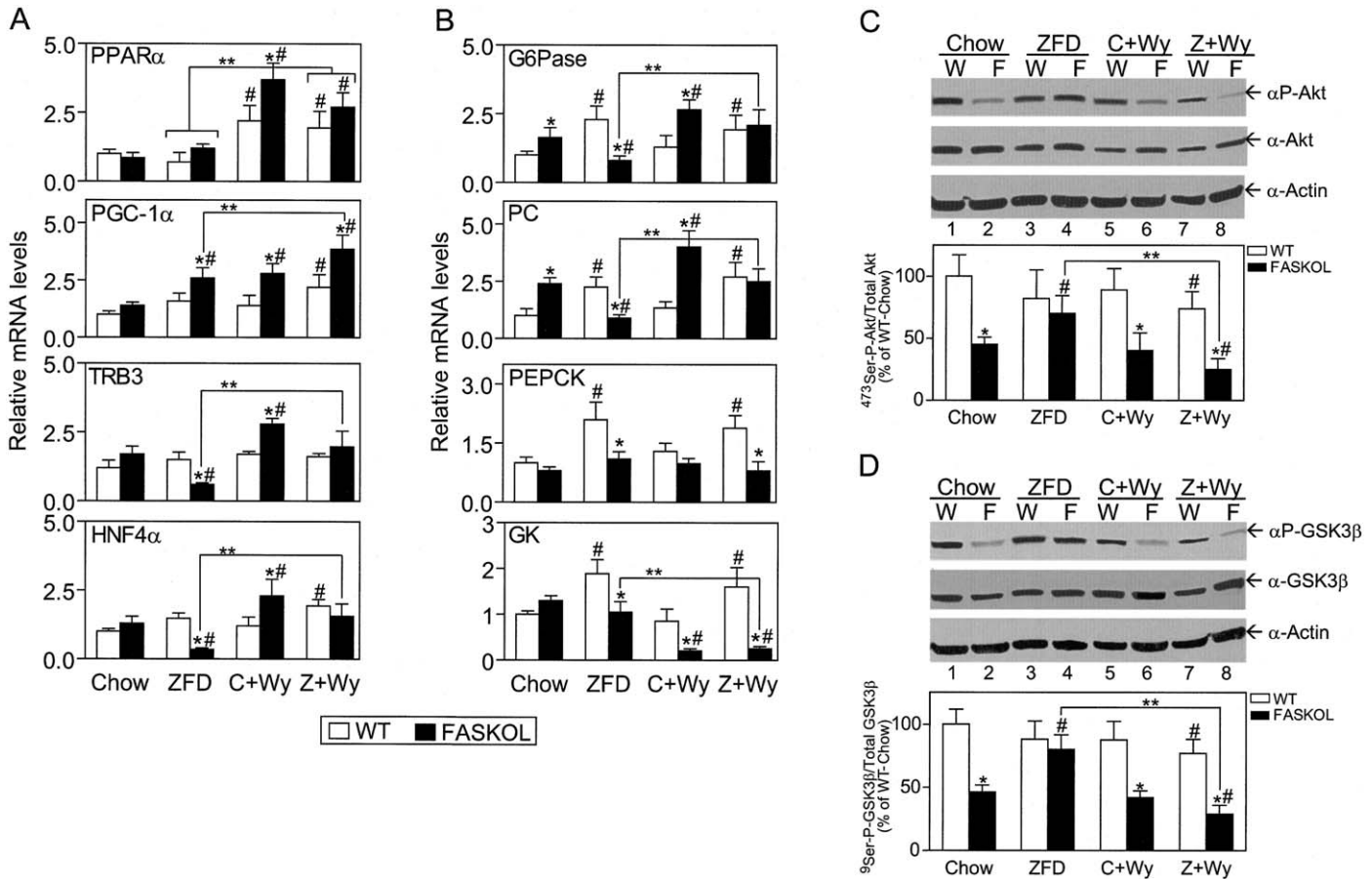
Figure 4. Expression of PPARα target genes and proteins involved in gluconeogenesis

A and B) Quantitative RT-PCR of RNA isolated from the livers of 4 hr fasted 16- to 20-week-old male wt (lox$^{+/+}$ Cre$^-$, white bars) and FASKOL (black bars) mice maintained on chow, ZFD for 10 days (ZFD), chow+Wy14,643 for 10 days (C+Wy), and ZFD+Wy14,643 for 10 days (Z+Wy). Data are mean ± SEM of three independent RT-PCR experiments for each gene with four mice of each genotype per dietary treatment for each experiment. Data are presented relative to *L32* ribosomal mRNA in the same samples and the relative mRNA levels were determined by QPCR using the comparative C_T method. $p < 0.05$ for the following: *, compared to the corresponding wt; #, compared to the corresponding chow-fed mice; **, compared to the corresponding ZFD-fed mice.

C and D) Immunoblot analysis of hepatic Akt (**C**) and GSK3β (**D**) from wt (W) and FASKOL (F) mice on the various diets as described in (**A**)–(**B**) above. Upper panels of (**C**) and (**D**) represent Akt phosphorylation on ^{473}Ser (αP-Akt) and GSK3β phosphorylation on ^{9}Ser (αP-GSK3β), respectively. Middle panels represent the total Akt and GSK3β proteins detected after stripping and reprobing the membranes with pan-Akt (α-Akt) and GSK3β (α-GSK3β) antibodies, respectively. The gels were scanned and quantified by densitometry. Intensities of the phosphorylated and total protein bands of wt mice on chow diet (control, lane 1) was arbitrarily set at 100%, and the relative intensities of the other bands were expressed relative to the control. Each bar represents mean ± SEM for 3–4 male wt and FASKOL mice. $p < 0.05$ for the following: *, compared to the corresponding wt; #, compared to the corresponding chow-fed mice; **, compared to the corresponding ZFD-fed mice.

2004), and *HNF4α*, another transcription factor coactivated by PGC-1α (Rhee et al., 2003), were both suppressed in ZFD-fed FASKOL livers and were significantly induced by PPARα activation with Wy in both the chow and ZFD in FASKOL livers (Figure 4A). Recent data from Yamamoto et al. (2004) imply that HNF4α expression is regulated by the insulin/glucagon ratio as well, through crosstalk with SREBP-1c and its interference with PGC-1α recruitment. HNF4α was shown to be absolutely required to induce gluconeogenic genes, as liver-specific HNF4α knockout mice had impaired induction of glucose 6-phosphatase (*G6Pase*) and phosphoenolpyruvate carboxykinase (*PEPCK*) even when PGC-1α was maximally activated (Rhee et al., 2003). Our results are consistent with these reports, with decreased expression of the gluconeogenic genes *G6Pase*, pyruvate carboxylase (*PC*), and *PEPCK* in ZFD-fed FASKOL livers (Figure 4B).

Carbohydrate feeding is known to increase gluconeogenic flux (Bizeau et al., 2001), explaining the increase in *G6Pase*, *PC*, and *PEPCK* expression with the ZFD in wt mice. The failure of this response, in concert with suppressed hepatic *HNF4α* despite a 3-fold induction of *PGC-1α*, provides a mechanism for the low glucose (Table 1; Figures 2A and 3A) in ZFD-fed FASKOL mice. Activation of PPARα with Wy in both chow and ZFD resulted in significant induction of *G6Pase* and *PC* above their respective baseline levels, but *PEPCK* was unaffected by Wy feeding (Figure 4B). This is consistent with previous reports, showing that *PEPCK* is not a PPARα target in liver (Kersten et al., 1999). Expression of *FOXO1*, another transcription factor required for PGC-1α-mediated induction of gluconeogenic genes (Puigserver et al., 2003), was also decreased in ZFD-fed FASKOL mice but did not increase with Wy compound (not shown).

Expression of glucokinase (*GK*) showed an appropriate expression pattern (Figure 4B) consistent with the low-insulin/high-glucagon hormonal milieu of the hypoglycemic ZFD-fed FASKOL mice. Carbohydrate feeding induces *GK* (Commerford et al., 2002). This response was attenuated in ZFD-fed FASKOL mice since *GK* mRNA levels were identical to those of chow-fed mice (Figure 4B). Incorporation of Wy in either chow or ZFD decreased *GK* expression in FASKOL but not wt liver (Figure 4B).

To further define the mechanisms underlying ZFD-induced hypoglycemia in FASKOL mice, Akt/PKB and glycogen synthase kinase 3-β (GSK3β), regulators of glucose and glycogen metabolism respectively, were analyzed in wt and FASKOL mice. There were no effects in skeletal muscle (not shown). ZFD feeding in FASKOL mice increased hepatic [473]serine-phosphorylated Akt (Figure 4C, lane 4) and [9]serine-phosphorylated GSK3β (Figure 4D, lane 4) compared to chow (lane 2, Figures 4C and 4D). Addition of Wy to chow and ZFD resulted in a marked decrease in the phosphorylated forms of Akt and GSK3β to levels similar to those seen with chow-only feeding (compare lanes 6 and 8 to lane 2, Figures 4C and 4D). These data suggest that enhanced hepatic insulin signaling in ZFD-fed FASKOL mice leads to decreased expression of gluconeogenic genes, ultimately causing hypoglycemia.

PPARα activation and the expression of fatty-acid and cholesterol metabolism genes

Similar to the striking changes in glucose-regulating genes, PPARα target genes critical for fatty-acid metabolism were decreased in ZFD-fed FASKOL livers (Figure 5A) and restored by pharmacological activation of PPARα. Expression of acyl-CoA oxidase (*ACO*), a peroxisomal fatty-acid oxidation enzyme and known PPARα target gene, was reduced by ∼50% in the livers of ZFD-fed FASKOL mice (Figure 5A) but was unaffected in kidney and heart (Figure S3B). As expected, *ACO* expression was increased to the same level as wt in liver (Figure 5A) as well as in kidney and heart (Figure S3B) when the Wy compound was combined with either the chow or ZFD. PPARα promotes ketone production. Expression of the mitochondrial enzyme HMG-CoA synthase-2 (*HS-2*), rate-limiting for hepatic ketogenesis and another known PPARα target gene, was decreased in ZFD-fed FASKOL mice and induced to the same level as wt when Wy was combined with ZFD but was almost 3-fold higher than wt with chow+Wy feeding (Figure 5A). The expression of liver fatty-acid binding protein (*L-FABP*), a PPARα target shown to physically interact with PPARα (Wolfrum et al., 2001), was reduced in ZFD-fed FASKOL livers, while it was increased in ZFD-fed wt livers compared to chow diet (Figure 5A). As expected for a PPARα target gene, it was induced with Wy feeding.

SREBP-1c expression was decreased in chow- and ZFD-fed FASKOL mice and was unaffected by Wy treatment compared to wt mice, consistent with the persistently low insulin levels in FASKOL mice (Figure 3B). *SREBP-1c* mRNA levels were unaffected by chow+Wy treatment but modestly decreased with ZFD+Wy feeding compared to ZFD alone (Figure 5A), likely reflecting the lower insulin in wt and FASKOL mice under these conditions (Figure 3B).

Lipoprotein lipase (*LPL*), a gene not normally expressed at high levels in adult liver but known to be induced by glucagon (Julve et al., 1996), was decreased in chow-fed FASKOL livers.

It was induced >40-fold with ZFD feeding in FASKOL mice (Figure 5A), which have high glucagon levels (Figure 3C). LPL is also known to be increased by PPARα ligands (Li et al., 2002), and its expression was induced 7- to 10-fold with chow+Wy feeding and 40- to 45-fold with ZFD+Wy feeding in both wt and FASKOL mice (Figure 5A). In contrast, carnitine palmitoyltransferase-1a (*CPT-1a*) was not affected in FASKOL livers under different feeding and ligand-treatment conditions (Figure 5A).

FASKOL mice had low levels of serum and hepatic cholesterol that were unaffected by the absence of dietary fat, and these levels were increased by PPARα activation (Figures 3I and 3J). To determine if decreased hepatic cholesterol content in this model was due to decreased cholesterol synthesis, increased excretion, or some combination of both, we analyzed the message levels for proteins mediating these processes. *SREBP-2* expression was increased in FASKOL liver (Figure 5B), the expected response to diminished intracellular cholesterol levels (Sato et al., 1996). *SREBP-2* is induced when the intracellular sterol content is low, stimulating the expression of genes required for cholesterol synthesis. Despite the appropriate induction of *SREBP-2*, the expression of *HMG-CoA reductase*, a major SREBP-2 target gene and the rate-limiting enzyme in cholesterol synthesis, was decreased in both chow- and ZFD-fed FASKOL mice (Figure 5B). The expression of insulin-induced gene 1 (*Insig-1*), which has been shown to inhibit cholesterol synthesis by blocking the proteolytic processing of SREBPs (Yang et al., 2002) and inducing proteosomal degradation of HMG-CoA reductase (Sever et al., 2003), was increased in chow- and ZFD-fed FASKOL livers compared to wt (Figure 5B). Hepatic cholesterol synthesis, determined in vivo using tritiated water, was reduced by more than 50% in both chow- and ZFD-fed FASKOL mice (Figure 5C). Treatment with the PPARα activator increased hepatic cholesterol biosynthesis by ∼2.5-fold, markedly reduced *Insig-1* expression (Figure 5B), increased *HMG-CoA reductase* expression (Figure 5B), increased hepatic cholesterol content (Figure 3J), and appropriately decreased *SREBP-2* expression (Figure 5B) in FASKOL mice.

The nuclear receptor LXRα and its target genes *ABCG5* and *ABCG8* are important regulators of cholesterol efflux (Repa et al., 2002). Steady-state levels of mRNA for *LXRα*, *ABCG5*, and *ABCG8* (Figure 5B), as well as *ABCA1* (not shown) were unaffected in FASKOL mice and did not change with diet or Wy treatment. The mRNA levels of two apoproteins, *apoB* and *apoE*, involved in cholesterol export were also unaffected (not shown). Collectively, these data suggest that disruption of FAS, regardless of dietary fat content, decreased hepatic cholesterol content by impairing cholesterol synthesis.

Prolonged fasting In FASKOL mice causes hypoglycemia, hepatic lipid accumulation, and decreased expression of PPARα target genes that are prevented by PPARα activation

To confirm the observation that hepatic deficiency of FAS interferes with PPARα activation, we used a different model than ZFD feeding. Mice were subjected to a 24 hr fast (Figure S4). FASKOL mice became hypoglycemic (Figure S4A), had decreased serum levels of the ketone β-HBA (Figure S4B), and had elevated circulating NEFA (Figure S4C), effects that were reversed by i.p. administration of the PPARα activator at the initiation of the fast. Increased liver triglyceride content in 24
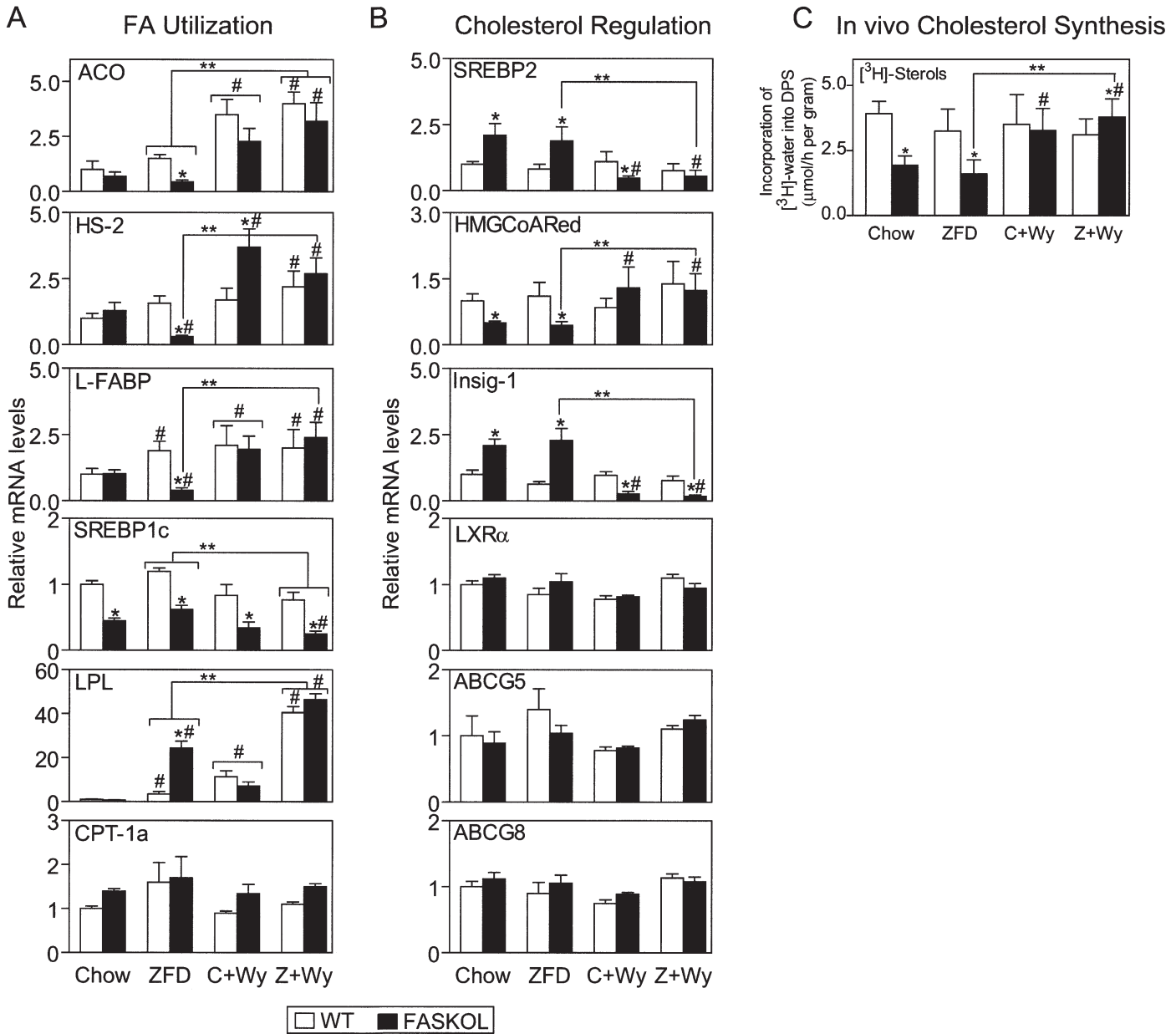
Figure 5. Expression of genes involved in lipid metabolism and measurement of in vivo liver cholesterol synthesis

A and B) Quantitative RT-PCR of RNA from livers of wt (lox$^{+/+}$ Cre$^-$, white bars) and FASKOL (black bars) mice fed chow, ZFD for 10 days (ZFD), chow+Wy14,643 for 10 days (C+Wy), and ZFD+Wy14,643 for 10 days (Z+Wy). Data are mean ± SEM of three independent RT-PCR experiments for each gene with four mice of each genotype per dietary treatment for each experiment. Data are presented relative to *L32* ribosomal mRNA in the same samples and the relative mRNA levels were determined by QPCR using the comparative C_T method. $p < 0.05$ for the following: *, compared to the corresponding wt; #, compared to the corresponding chow-fed mice; **, compared to the corresponding ZFD-fed mice.

C) Hepatic cholesterol synthesis rates were determined in wt (white bars) and FASKOL (black bars) mice fed the various diets as described in (**A**) and (**B**) above using ^{3}H-water. Incorporation of ^{3}H-radioactivity into digitonin-precipitable sterols (DPS) was expressed as µmoles per hour per gram of tissue. Each bar represents the mean ± SEM of 3–5 male mice per genotype per dietary treatment. $p < 0.05$ for the following: *, compared to the corresponding wt; #, compared to the corresponding chow-fed mice; **, compared to the corresponding ZFD-fed mice.

hr fasted FASKOL mice was also prevented by Wy compound (Figure S4D).

Gene expression in FASKOL mice subjected to the prolonged fast mirrored that of ZFD-fed animals. Although *PPARα*, *PGC-1α*, and *TRB3* message levels were unaffected by genotype after a 24 hr fast, only the latter two genes were preferen-tially induced by Wy injection in the FASKOL mice, while *PPARα* expression was increased by Wy in both wt and FASKOL mice (Figure S4E). The expression of *HNF4α* in FASKOL livers after a 24 hr fast was similar to that seen in ZFD-fed FASKOL livers and was significantly induced by Wy (Figure S4E). The mRNA levels of cAMP response element

binding protein (*CREB*), regulated in the fasting state by glucagon, were higher in 24 hr fasted FASKOL mice with and without Wy injection, compared to wt (Figure S4E). *CPT-1a* was lower in 24 hr fasted FASKOL livers (Figure S4F), different from the response in ZFD-fed FASKOL mice (Figure 5A), and unaffected by Wy administration. Expression of *ACO*, *HS-2*, *PC*, and *G6Pase* (Figure S4F), PPARα target genes involved in fatty-acid oxidation, ketogenesis, and gluconeogenesis, was decreased after a 24 hr fast in FASKOL mice, mirroring the expression patterns seen in ZFD-fed FASKOL mice, and all were induced to wt levels when the PPARα activator was injected at the initiation of the fast (Figure S4F).

Discussion

A model for differential effects of new versus old fat in liver

Fatty acids can serve as signaling molecules (Pegorier et al., 2004), especially in the liver, where perturbations of normal nutrient homeostasis in conditions such as insulin resistance, diabetes, and obesity result in the accelerated production of glucose and atherogenic lipoproteins, common contributors to human disease. In this paper, we show that the source of these fatty acids is critical for maintaining normal glucose, lipid, and cholesterol metabolism.

When FASKOL mice (lacking the capacity to synthesize fatty acids from carbohydrate) were fed a diet without fat, they developed hypoglycemia and fatty liver in the setting of decreased expression of PPARα target genes (Table 1; Figures 2–5). The same effects were seen when FASKOL mice were subjected to prolonged fasting (Figure S4), as in PPARα-deficient mice. Malonyl-CoA participates in the regulation of fatty-acid oxidation but is unlikely to mediate the FASKOL phenotype since differences in malonyl-CoA were unaffected by diet (Results). The hypoglycemia/steatohepatitis phenotype and defects in PPARα target gene expression were corrected by administration of a potent PPARα agonist (Figures 3–5 and Figure S4). FASKOL mice also had a cholesterol phenotype that, unlike the development of hypoglycemia/steatohepatitis, was not dependent on diet. Regardless of the availability of dietary fat, serum and hepatic cholesterol levels were low in FASKOL mice in association with increased *SREBP-2*, decreased *HMG-CoA reductase* gene expression, and decreased hepatic cholesterol synthesis (Figures 3 and 5). These effects were also normalized by pharmacologically activating PPARα (Figures 3 and 5). Thus, the metabolic abnormalities in FASKOL mice appear to be driven by the failure to activate available PPARα. PPARα⁻/⁻ mice did not develop a phenotype with ZFD feeding (Figure S2).

Our results are consistent with the model shown in Figure 6 indicating that new fatty acids are the endogenous activators of physiologically distinct pools of PPARα. FASKOL mice are protected from the hypoglycemia/steatohepatitis phenotype when new fat absorbed from the diet (D in Figure 6) is available to activate one pool of PPARα and promote gluconeogenesis (GNEO) as well as fatty-acid oxidation (FAO). Regardless of diet, FASKOL mice have low hepatic stores of cholesterol that are normalized by PPARα activation, suggesting that new fat produced by FAS (N in Figure 6) has access to a separate pool of PPARα capable of stimulating cholesterol biosynthesis (CHOL) in addition to gluconeogenesis and fatty-acid oxidation. New fat synthesized by FAS may be the preferred endogenous PPARα activator. Even in the presence of dietary fat, FASKOL mice tend to have lower glucose levels, insulin levels are significantly lower (Table 1), and mRNA levels for the gluconeogenic enzymes G6Pase and PC (Figure 4B) are significantly induced, suggesting the need for increased gluconeogenesis (perhaps driven by dietary fat) in the absence of FAS. Over time, ZFD-fed FASKOL mice mobilize peripheral fat stores and transport this lipid to the liver where it accumulates (old fat in Figure 6). But this lipid source fails to activate PPARα, blood glucose and cholesterol levels remain low, and steatohepatitis progresses. Thus, specific fatty-acid pools synthesized by hepatic FAS or derived from the diet, but not those stored in the liver after transfer from the periphery (even when present in abundance), activate PPARα to impact glucose and lipid metabolism. While these observations establish the existence of distinct physiological lipid compartments, identification of the precise subcellular location of these compartments will require additional studies.

FASKOL mice and the disruption of cholesterol metabolism

Impaired activation of PPARα is a feasible cause of the hypoglycemia/fatty-liver phenotype in our mice since this ligand-activated transcription factor is known to play important roles in gluconeogenesis (Bernal-Mizrachi et al., 2003; Koo et al., 2004), fatty-acid oxidation (Reddy, 2001), and ketogenesis (Rodriguez et al., 1994). FASKOL mice also had abnormal cholesterol metabolism, characterized by decreased activation of a critical SREBP-2 target gene (*HMG-CoA reductase*), that was corrected by treatment with a PPARα agonist. There is precedence for the involvement of PPARα and peroxisomes in cholesterol metabolism. Peroxisome-deficient PEX2 null mice have a complex cholesterol phenotype (Kovacs et al., 2004). Hepatic cholesterol content is decreased, *SREBP-2* mRNA is increased, *SREBP-1c* is decreased, and LXR target genes are not activated, effects also seen in FASKOL mice. In whole-body PPARα null mice, hepatic cholesterol and *HMG-CoA reductase* expression are decreased (Patel et al., 2001). PPARα activators have been reported to increase *HMG-CoA reductase* gene expression in hepatocytes (Le Jossic-Corcos et al., 2004). Viewed together, these data suggest that normal peroxisomal function is required to maintain cholesterol homeostasis.

Cholesterol metabolism in FASKOL mice shares some features with transgenic mice overexpressing Insig-1 in liver (Engelking et al., 2004) and liver-specific HNF4α knockout mice (Hayhurst et al., 2001). Insigs are ER proteins that, in the presence of sterols, bind to HMG-CoA reductase and SCAP, an escort protein required for the generation of transcriptionally active SREBPs. Insig-1 liver transgenics have decreased plasma and hepatic cholesterol, decreased activation of SREBP-2 target genes such as *HMG-CoA reductase*, and no effect on LXR or its target genes, resembling FASKOL mice. Liver-specific HNF4α knockout mice have decreased plasma cholesterol, fatty liver, decreased expression of *PPARα* as well as *L-FABP*, and normal *LXRα* expression, as in FASKOL mice. These data suggest that PPARα signaling through products of the FAS reaction facilitates SREBP processing and HNF4α activation.
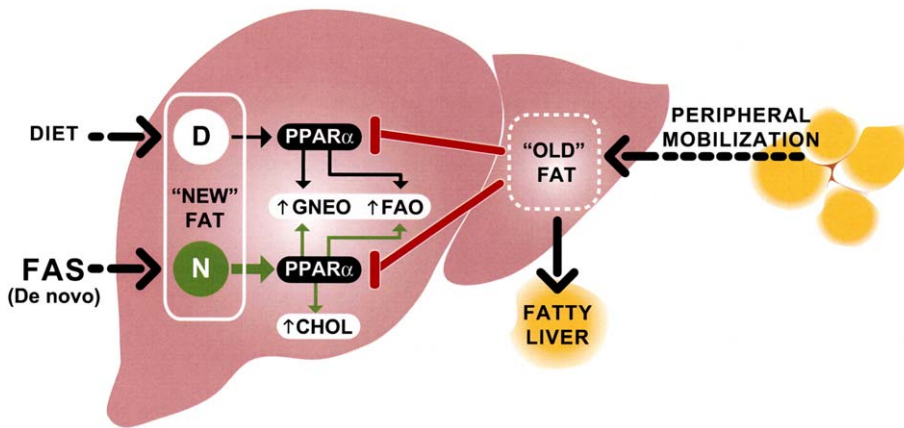
Figure 6. Model for differential effects of hepatic lipid

Fat absorbed from the diet or synthesized de novo via FAS in the liver constitutes "new" fat, capable of activating PPARα to ensure normal glucose and lipid homeostasis. Fat derived from peripheral mobilization of adipose stores constitutes a different hepatic compartment ("old" fat) that does not appear to activate PPARα as effectively as new fat, leading to fatty liver. In contrast to de novo synthesized fat, dietary fat is inadequate for the maintenance of cholesterol homeostasis, suggesting different PPARα pools.

Is FAS-derived palmitate the endogenous activator of PPARα?

Our results provide evidence that hepatic FAS is necessary for the normal activation of PPARα target genes but do not provide definitive identification of the responsible ligand. The saturated fatty acid palmitate (16:0) is the major product of the FAS reaction, and palmitate levels were decreased in FASKOL liver (Figure 1). Although unsaturated fatty acids are generally considered to be the endogenous ligands for PPARs, several lines of evidence suggest that palmitate or related FAS products activate PPARα. Palmitate as well as laurate (12:0) and stearate (18:0) have been shown to transactivate PPARα using reporter gene constructs (Kliewer et al., 1997; Gottlicher et al., 1992). Palmitate, myristate (14:0), and stearate each bind to PPARα with an affinity similar to that of some unsaturated fatty acids (Xu et al., 1999). Physiologically, saturated fatty acids stimulate both gluconeogenesis (Bizeau et al., 2001) and cholesterol synthesis (Glatz and Katan, 1993), processes associated with PPARα activation. HNF4α shows constitutive binding of saturated as well as unsaturated C14-C18 fatty acids (Wisely et al., 2002). It is thus plausible that FAS products could affect gene expression by binding and activating PPARα.

How is new fat compartmentalized to activate PPARα?

The observation that new fat has specific metabolic effects implies the existence of discrete physiological compartments. FAS is a cytosolic enzyme and PPARα, when it activates gene expression, is in the nucleus. How is the product of a cytosolic enzyme delivered to a nuclear factor? How does the cell distinguish between newly absorbed and stored fat? One possibility is that lipid binding proteins specific for new fat shuttle fatty acids to nuclear PPARα. Liver fatty-acid binding protein (L-FABP) is present in both cytosol and nucleus and interacts with PPARα (Wolfrum et al., 2001). However, PPARα target gene expression is largely preserved in L-FABP null mice (Newberry et al., 2003; Erol et al., 2004). Another possibility is that PPARα shuttles between the nucleus and the cytoplasm with the assistance of chaperones that promote an interaction with the new fat pool. In support of this notion, cytosolic PPARα was recently shown to be stably associated with the chaperone protein hsp90 (Sumanasekera et al., 2003a; Sumanasekera et al., 2003b).

In short, all fatty acids are not created equal, at least in the hepatocyte. De novo lipogenesis mediated by FAS plays a regulatory role in glucose, lipid, and cholesterol metabolism by providing an endogenous ligand for activation of PPARα. Defining the process by which new fat is preferentially delivered to PPARα could have important implications for understanding how nuclear receptor family members that serve as nutrient sensors distinguish between different sources of fatty acids.

Experimental procedures

Animals

A 9.3 kb HindIII fragment including exons 1–9 of the mouse FAS gene was isolated from a mouse BAC clone (129/SvJ). A combination of conventional cloning and long-distance PCR was used to generate the targeting vector shown in Figure 1A. RW-4 embryonic stem cells were electroporated at the Washington University ES Core, and 5 of 191 screened colonies were found to be correctly targeted. One clone (C12) was injected into C57BL/6 blastocysts to generate chimeric mice. Floxed, germline offspring were crossed with albumin-Cre mice (Postic and Magnuson, 2000) or EIIaCre mice (Lakso et al., 1996). The Washington University Animal Care Committee approved these experiments.

Mice were genotyped by PCR using FAS-specific primers (5′-ATGTCTGG TTGTTCTTGGGCTGA-3′ and 5′-GGTCATCGAGACAACCACACAT-3′) and Cre-specific primers (5′-GCGGTCTGGCAGTAAAAACTATC-3′ and 5′-GTG AAACAGCATTGCTGTCACTT-3′). For Southern blotting, genomic DNA was isolated using DNAEasy Kit (Invitrogen), digested with NdeI and HindIII, and detected using Probe C in Figure 1A.

All experiments were performed at 16–20 weeks of age to allow for maximal effects of albumin-Cre. Animals were fed a standard mouse chow diet (Purina 5053) with a total fat content of 4.5%, protein content of 22%, and 45%–55% nitrogen-free excess (which includes carbohydrates) by weight, yielding a total caloric value of ∼3.0 kcal/g. The zero-fat diet (ZFD) (Harlan Teklad, TD 03314) consisted of 0% fat, 20% protein, and 63% carbohydrates by weight, yielding a total caloric value of 3.3 kcal/g (24% protein/ 76% carbohydrate by caloric content). This diet is well tolerated in rodents (Iritani et al., 2000). In some experiments, animals were fed either chow or ZFD containing the PPARα agonist Wy14,643 (TD 03579). For this diet, Wy14,643 (Biomol Research Laboratories) was shipped directly to the supplier and incorporated into standard rodent chow P5053 (Chow+Wy) or TD 03314 (ZFD+Wy) both at 0.1% (wt/wt). Experimental animals were weighed weekly. Food intake was determined in individually housed mice by weighing remaining diet and accounting for spillage using metabolic cages. For 24 hr fasting studies, food was withdrawn at the beginning of the light cycle, and mice were injected intraperitoneally with Wy14,643 (50 μg/g in 30% DMSO) or vehicle alone (30% DMSO) as described (Pedraza et al., 2000).

Analytical procedures

Triglycerides, cholesterol, glucose, nonesterifed fatty acids (NEFA), and insulin were assayed as described (Marshall et al., 1999; Li et al., 2000). Leptin and adiponectin were assayed by ELISA using commercial reagents (CrystalChem, R&D Systems). Glucagon and C peptide radioimmunoassays as well as determinations of ALT (alanine aminotransferase), bilirubin, alkaline phosphatase, albumin, lactate, and β-hydroxybutyrate were performed in mouse core facilities at Washington University. Body composition and indirect calorimetry were performed as described (Bernal-Mizrachi et al., 2002). Glucose-tolerance and insulin-tolerance tests were performed as described (Li et al., 2000).

FAS enzyme activity and malonyl-CoA content

FAS enzyme activity was determined using a modification of a previously described assay (Ullman and White, 1981). Freshly harvested tissues were weighed and homogenized in 0.1 M potassium phosphate buffer (pH 7.0), containing 8% sucrose, 1 mM EDTA (pH 8.0), and 20 mM 2-mercaptoethanol at 4°C. Homogenates were centrifuged at 3,000 × g for 10 min at 4°C. Ten microliters of the supernatant was added to 80 μl of assay buffer (2 mM EDTA [pH 8.0], 2 mM DTT, 0.4 mg/ml NADPH), and the rate of NADPH oxidation was monitored at 340 nm. The substrate-dependent rate was determined by subtracting the NADPH oxidation rate from the rate after adding 10 μl of 0.85 mg/ml of malonyl-CoA (Sigma).

Malonyl-CoA was determined in extracts homogenized in deionized water. CoA esters were separated using reversed-phase HPLC on a 5 μm Supelco C18 column with a Waters HPLC system, monitoring 254 nm as the maximal absorbance for CoA. Buffers, gradients, and flow rates were those described previously (Pizer et al., 2000).

Gas chromatography-mass spectrometry (GC-MS)

Samples were analyzed as described (Turk et al., 1986; Wolf et al., 1991). Fifty milligram aliquots of frozen liver were homogenized in 3 ml of 2:1 (v/v) chloroform:methanol and the organic phase isolated. Thirty microliters of each extract was saponified in 1.0 ml of 5 mM KOH in ethanol for 2 hr at 100°C followed by treatment with 100 μl 1.2 N HCl and 2.5 ml of ethyl acetate. The organic phase was derivatized to methyl esters by the addition of 100 μl HCl:methanol (1:3 v/v) and heating at 70°C for 1 hr. The derivatized samples were reconstituted in hexane and analyzed on a Varian 3400 gas chromatograph interfaced to a Finnegan SSQ 7000 mass spectrometer. Samples were analyzed at injector and transfer line temperatures of 250°C and ionization was achieved by electron impact. Selected ion monitoring was used at mass-to-charge ratio (m/z) of 270 and 274 for the methyl esters of native palmitate and of the 5,5,6,6-palmitic acid-d4 internal standard, respectively. The ratio of the ion current at m/z 270 and 274 was used to determine the amount of palmitate by interpolation from a standard curve.

Hepatic assays and histology

Frozen aliquots (25–30 mg) of liver were homogenized in chloroform:methanol (2:1 vol/vol) and extracts analyzed using ThermoDMA triglyceride and cholesterol reagents (Thermoelectron Corp.). Perchloric acid extracts of liver were assayed for glycogen by the amyloglucosidase method (Passonneau and Lauderdale, 1974). For histology, some livers were fixed in 10% neutral buffered formalin and embedded in paraffin, and 4–6 μm sections were cut and stained with hematoxylin and eosin (H&E). Other livers were fixed in alcoholic formalin or frozen in Tissue-Tek OCT (Miles, Inc.) for determination of glycogen and neutral lipids by periodic acid-schiff (PAS) and ORO staining, respectively.

In vivo cholesterol synthesis

Rates of liver cholesterol synthesis were measured in 16- to 24-week-old FASKOL and wt littermates during the early light cycle after a 2 hr fast on the various dietary regimens (4–5 mice per genotype per dietary treatment group) using [3H]-labeled water as previously described (Shimano et al., 1996). Each animal was injected intraperitoneally with 50 mCi of [3H]-water in 0.2 ml of saline. One hour after injection, 300–500 μl of blood was drawn from the inferior vena cava to determine the plasma [3H]-water-specific activity in duplicate. The livers were then removed, and 200–300 mg portions were processed as previously described (Dietschy and Spady, 1984). The rates of cholesterol synthesis were calculated as μmoles of [3H]-radioactivity incorporated into digitonin-precipitable sterols (DPS) per hour per gram of tissue (Spady and Dietschy, 1983).

Quantitative RT-PCR-based gene expression

Total RNA was extracted with TRIzol reagent (Invitrogen). There was no effect of genotype on RNA yields. After treatment with DNaseI, 1 μg of total RNA was reverse transcribed with an oligo-dT primer, and then quantitative PCR was performed with the ABI Prism7700 PCR instrument (Applied Biosystems) using the TaqMan Universal PCR Master Mix reagent kit. Each assay included a negative control using RNA not subjected to reverse transcription. Oligonucleotide primers and TaqMan probes were designed using Primer Express software (Applied Biosystems). Sequences are shown in Table S1. Amplification specificity was verified by assessing products on an agarose gel and using a heat-dissociation protocol. Sequence-specific amplification was detected with an increasing fluorescent signal of FAM (reporter dye) during the amplification cycle. Coamplification of the mRNA for the mouse ribosomal protein L32 was performed in all samples. Assays were performed in triplicate and results normalized to *L32* mRNA levels, which were unaffected by genotype or diet. Message levels were also normalized to another invariant internal control, acidic ribosomal phosphoprotein 36B4, with similar results to that seen with L32.

Western blotting

Livers and skeletal muscle (gastrocnemius) were frozen and homogenized at 4°C as described previously (Kerouz et al., 1997). Thirty micrograms of protein were resolved on a 10% SDS-polyacrylamide gel, electrotransferred onto PVDF membranes (Amersham). Membranes were incubated with rabbit anti-mouse phospho-Akt (recognizing phosphorylated Akt at serine 473, Cell Signaling 9271) and rabbit anti-mouse phospho-GSK3β (recognizing phosphorylated GSK3b at serine 9, Cell signaling 9336) at 1:1000 dilution at 4°C overnight, followed by secondary antibody incubation at 1:7500 dilution for 1 hr. Phospho-Akt- and phospho-GSK3β-specific bands were detected by chemiluminescence (ECL kit, Amersham), then membranes were stripped and reprobed with rabbit anti-mouse pan-Akt (recognizing total Akt protein, Cell Signaling 9272) and rabbit anti-mouse pan-GSK3β (recognizing total GSK3β protein, Cell Signaling 9332) also at 1:1000 dilution at 4°C overnight. Reprobing with anti-actin antibody (Sigma, A2066) was performed to ensure equal loading of protein in all lanes.

Statistical analyses

Values are expressed as mean ± standard error of the mean (SEM). Statistical comparisons were performed using an unpaired, two-tailed Student's t test (when two groups were analyzed) or analysis of variance (ANOVA). If the overall F was found to be significant for the latter, comparisons between means were made using appropriate post-hoc tests.

Supplemental data

Supplemental data include four figures and one table and can be found with this article online at http://www.cellmetabolism.org/cgi/content/full/1/5/309/DC1/.

References

Berger, J., and Moller, D.E. (2002). The mechanisms of action of PPARs. Annu. Rev. Med. *53*, 409–435.

Bernal-Mizrachi, C., Weng, S., Li, B., Nolte, L.A., Feng, C., Coleman, T., Holloszy, J.O., and Semenkovich, C.F. (2002). Respiratory uncoupling lowers blood pressure through a leptin-dependent mechanism in genetically obese mice. Arterioscler. Thromb. Vasc. Biol. 22, 961–968.

Bernal-Mizrachi, C., Weng, S., Feng, C., Finck, B.N., Knutsen, R.H., Leone, T.C., Coleman, T., Mecham, R.P., Kelly, D.P., and Semenkovich, C.F. (2003). Dexamethasone induction of hypertension and diabetes is PPAR-alpha dependent in LDL receptor-null mice. Nat. Med. 9, 1069–1075.

Bizeau, M.E., Short, C., Thresher, J.S., Commerford, S.R., Willis, W.T., and Pagliassotti, M.J. (2001). Increased pyruvate flux capacities account for diet-induced increases in gluconeogenesis in vitro. Am. J. Physiol. Regul. Integr. Comp. Physiol. 281, R427–R433.

Chen, G., Liang, G., Ou, J., Goldstein, J.L., and Brown, M.S. (2004). Central role for liver X receptor in insulin-mediated activation of SREBP-1c transcription and stimulation of fatty acid synthesis in liver. Proc. Natl. Acad. Sci. USA 101, 11245–11250.

Chirala, S.S., Chang, H., Matzuk, M., Abu-Elheiga, L., Mao, J., Mahon, K., Finegold, M., and Wakil, S.J. (2003). Fatty acid synthesis is essential in embryonic development: fatty acid synthase null mutants and most of the heterozygotes die in utero. Proc. Natl. Acad. Sci. USA 100, 6358–6363.

Commerford, S.R., Ferniza, J.B., Bizeau, M.E., Thresher, J.S., Willis, W.T., and Pagliassotti, M.J. (2002). Diets enriched in sucrose or fat increase gluconeogenesis and G-6-Pase but not basal glucose production in rats. Am. J. Physiol. Endocrinol. Metab. 283, E545–E555.

Dietschy, J.M., and Spady, D.K. (1984). Measurement of rates of cholesterol synthesis using tritiated water. J. Lipid Res. 25, 1469–1476.

Engelking, L.J., Kuriyama, H., Hammer, R.E., Horton, J.D., Brown, M.S., Goldstein, J.L., and Liang, G. (2004). Overexpression of Insig-1 in the livers of transgenic mice inhibits SREBP processing and reduces insulin-stimulated lipogenesis. J. Clin. Invest. 113, 1168–1175.

Erol, E., Kumar, L.S., Cline, G.W., Shulman, G.I., Kelly, D.P., and Binas, B. (2004). Liver fatty acid binding protein is required for high rates of hepatic fatty acid oxidation but not for the action of PPARalpha in fasting mice. FASEB J. 18, 347–349.

Glatz, J.F., and Katan, M.B. (1993). Dietary saturated fatty acids increase cholesterol synthesis and fecal steroid excretion in healthy men and women. Eur. J. Clin. Invest. 23, 648–655.

Gottlicher, M., Widmark, E., Li, Q., and Gustafsson, J.A. (1992). Fatty acids activate a chimera of the clofibric acid-activated receptor and the glucocorticoid receptor. Proc. Natl. Acad. Sci. USA 89, 4653–4657.

Hayhurst, G.P., Lee, Y.H., Lambert, G., Ward, J.M., and Gonzalez, F.J. (2001). Hepatocyte nuclear factor 4alpha (nuclear receptor 2A1) is essential for maintenance of hepatic gene expression and lipid homeostasis. Mol. Cell. Biol. 21, 1393–1403.

Horton, J.D., Goldstein, J.L., and Brown, M.S. (2002). SREBPs: activators of the complete program of cholesterol and fatty acid synthesis in the liver. J. Clin. Invest. 109, 1125–1131.

Iritani, N., Sugimoto, T., and Fukuda, H. (2000). Gene expression of leptin, insulin receptors, and lipogenic enzymes are coordinately regulated by insulin and dietary fat in rats. J. Nutr. 130, 1183–1188.

Julve, J., Robert, M.Q., Llobera, M., and Peinado-Onsurbe, J. (1996). Hormonal regulation of lipoprotein lipase activity from 5-day-old rat hepatocytes. Mol. Cell. Endocrinol. 116, 97–104.

Jump, D.B., and Clarke, S.D. (1999). Regulation of gene expression by dietary fat. Annu. Rev. Nutr. 19, 63–90.

Kerouz, N.J., Horsch, D., Pons, S., and Kahn, C.R. (1997). Differential regulation of insulin receptor substrates-1 and -2 (IRS-1 and IRS-2) and phosphatidylinositol 3-kinase isoforms in liver and muscle of the obese diabetic (ob/ob) mouse. J. Clin. Invest. 100, 3164–3172.

Kersten, S., Seydoux, J., Peters, J.M., Gonzalez, F.J., Desvergne, B., and Wahli, W. (1999). Peroxisome proliferator-activated receptor alpha mediates the adaptive response to fasting. J. Clin. Invest. 103, 1489–1498.

Kliewer, S.A., Sundseth, S.S., Jones, S.A., Brown, P.J., Wisely, G.B., Koble, C.S., Devchand, P., Wahli, W., Willson, T.M., Lenhard, J.M., et al. (1997). Fatty acids and eicosanoids regulate gene expression through direct interactions with peroxisome proliferator-activated receptors alpha and gamma. Proc. Natl. Acad. Sci. USA 94, 4318–4323.

Koo, S.H., Satoh, H., Herzig, S., Lee, C.H., Hedrick, S., Kulkarni, R., Evans, R.M., Olefsky, J., and Montminy, M. (2004). PGC-1 promotes insulin resistance in liver through PPAR-alpha-dependent induction of TRB-3. Nat. Med. 10, 530–534.

Kovacs, W.J., Shackelford, J.E., Tape, K.N., Richards, M.J., Faust, P.L., Fliesler, S.J., and Krisans, S.K. (2004). Disturbed cholesterol homeostasis in a peroxisome-deficient PEX2 knockout mouse model. Mol. Cell. Biol. 24, 1–13.

Lakso, M., Pichel, J.G., Gorman, J.R., Sauer, B., Okamoto, Y., Lee, E., Alt, F.W., and Westphal, H. (1996). Efficient in vivo manipulation of mouse genomic sequences at the zygote stage. Proc. Natl. Acad. Sci. USA 93, 5860–5865.

Langhans, W. (2003). Role of the liver in the control of glucose-lipid utilization and body weight. Curr. Opin. Clin. Nutr. Metab. Care 6, 449–455.

Latruffe, N., and Vamecq, J. (2000). Evolutionary aspects of peroxisomes as cell organelles, and of genes encoding peroxisomal proteins. Biol. Cell. 92, 389–395.

Le Jossic-Corcos, C., Duclos, S., Ramirez, L.C., Zaghini, I., Chevillard, G., Martin, P., Pineau, T., and Bournot, P. (2004). Effects of peroxisome proliferator-activated receptor alpha activation on pathways contributing to cholesterol homeostasis in rat hepatocytes. Biochim. Biophys. Acta 1683, 49–58.

Li, B., Nolte, L.A., Ju, J.S., Han, D.H., Coleman, T., Holloszy, J.O., and Semenkovich, C.F. (2000). Skeletal muscle respiratory uncoupling prevents diet-induced obesity and insulin resistance in mice. Nat. Med. 6, 1115–1120.

Li, L., Beauchamp, M.C., and Renier, G. (2002). Peroxisome proliferator-activated receptor alpha and gamma agonists upregulate human macrophage lipoprotein lipase expression. Atherosclerosis 165, 101–110.

Marshall, B.A., Tordjman, K., Host, H.H., Ensor, N.J., Kwon, G., Marshall, C.A., Coleman, T., McDaniel, M.L., and Semenkovich, C.F. (1999). Relative hypoglycemia and hyperinsulinemia in mice with heterozygous lipoprotein lipase (LPL) deficiency. Islet LPL regulates insulin secretion. J. Biol. Chem. 274, 27426–27432.

Newberry, E.P., Xie, Y., Kennedy, S., Han, X., Buhman, K.K., Luo, J., Gross, R.W., and Davidson, N.O. (2003). Decreased hepatic triglyceride accumulation and altered fatty acid uptake in mice with deletion of the liver fatty acid-binding protein gene. J. Biol. Chem. 278, 51664–51672.

Passonneau, J.V., and Lauderdale, V.R. (1974). A comparison of three methods of glycogen measurement in tissues. Anal. Biochem. 60, 405–412.

Patel, D.D., Knight, B.L., Wiggins, D., Humphreys, S.M., and Gibbons, G.F. (2001). Disturbances in the normal regulation of SREBP-sensitive genes in PPAR alpha-deficient mice. J. Lipid Res. 42, 328–337.

Patsouris, D., Mandard, S., Voshol, P.J., Escher, P., Tan, N.S., Havekes, L.M., Koenig, W., Marz, W., Tafuri, S., Wahli, W., et al. (2004). PPARalpha governs glycerol metabolism. J. Clin. Invest. 114, 94–103.

Pawar, A., Botolin, D., Mangelsdorf, D.J., and Jump, D.B. (2003). The role of liver X receptor-alpha in the fatty acid regulation of hepatic gene expression. J. Biol. Chem. 278, 40736–40743.

Pedraza, N., Solanes, G., Carmona, M.C., Iglesias, R., Vinas, O., Mampel, T., Vazquez, M., Giralt, M., and Villarroya, F. (2000). Impaired expression of the uncoupling protein-3 gene in skeletal muscle during lactation: fibrates and troglitazone reverse lactation-induced downregulation of the uncoupling protein-3 gene. Diabetes 49, 1224–1230.

Pegorier, J.P., Le May, C., and Girard, J. (2004). Control of gene expression by fatty acids. J. Nutr. 134, 2444S–2449S.

Pizer, E.S., Thupari, J., Han, W.F., Pinn, M.L., Chrest, F.J., Frehywot, G.L., Townsend, C.A., and Kuhajda, F.P. (2000). Malonyl-coenzyme A is a potential mediator of cytotoxicity induced by fatty acid synthase in human breast cancer cells and xenografts. Cancer Res. 60, 213–218.

Postic, C., and Magnuson, M.A. (2000). DNA excision in liver by an albumin-Cre transgene occurs progressively with age. Genesis 26, 149–150.

Puigserver, P., Rhee, J., Donovan, J., Walkey, C.J., Yoon, J.C., Oriente, F., Kitamura, Y., Altomonte, J., Dong, H., Accili, D., and Spiegelman, B.M. (2003). Insulin-regulated hepatic gluconeogenesis through FOXO1-PGC-1alpha interaction. Nature 423, 550–555.

Reddy, J.K. (2001). Nonalcoholic steatosis and steatohepatitis. III. Peroxisomal beta-oxidation, PPAR alpha, and steatohepatitis. Am. J. Physiol. Gastrointest. Liver Physiol. 281, G1333–G1339.

Repa, J.J., Berge, K.E., Pomajzl, C., Richardson, J.A., Hobbs, H., and Mangelsdorf, D.J. (2002). Regulation of ATP-binding cassette sterol transporters ABCG5 and ABCG8 by the liver X receptors alpha and beta. J. Biol. Chem. 277, 18793–18800.

Rhee, J., Inoue, Y., Yoon, J.C., Puigserver, P., Fan, M., Gonzalez, F.J., and Spiegelman, B.M. (2003). Regulation of hepatic fasting response by PPAR-gamma coactivator-1alpha (PGC-1): requirement for hepatocyte nuclear factor 4alpha in gluconeogenesis. Proc. Natl. Acad. Sci. USA 100, 4012–4017.

Rodriguez, J.C., Gil-Gomez, G., Hegardt, F.G., and Haro, D. (1994). Peroxisome proliferator-activated receptor mediates induction of the mitochondrial 3-hydroxy-3-methylglutaryl-CoA synthase gene by fatty acids. J. Biol. Chem. 269, 18767–18772.

Sato, R., Inoue, J., Kawabe, Y., Kodama, T., Takano, T., and Maeda, M. (1996). Sterol-dependent transcriptional regulation of sterol regulatory element-binding protein-2. J. Biol. Chem. 271, 26461–26464.

Semenkovich, C.F. (1997). Regulation of fatty acid synthase (FAS). Prog. Lipid Res. 36, 43–53.

Sever, N., Yang, T., Brown, M.S., Goldstein, J.L., and DeBose-Boyd, R.A. (2003). Accelerated degradation of HMG CoA reductase mediated by binding of insig-1 to its sterol-sensing domain. Mol. Cell 11, 25–33.

Shimano, H., Horton, J.D., Hammer, R.E., Shimomura, I., Brown, M.S., and Goldstein, J.L. (1996). Overproduction of cholesterol and fatty acids causes massive liver enlargement in transgenic mice expressing truncated SREBP-1a. J. Clin. Invest. 98, 1575–1584.

Spady, D.K., and Dietschy, J.M. (1983). Sterol synthesis in vivo in 18 tissues of the squirrel, monkey, guinea pig, rabbit, hamster, and rat. J. Lipid Res. 24, 303–315.

Sumanasekera, W.K., Tien, E.S., Davis, J.W., 2nd, Turpey, R., Perdew, G.H., and Vanden Heuvel, J.P. (2003a). Heat shock protein-90 (Hsp90) acts as a repressor of peroxisome proliferator-activated receptor-alpha (PPARalpha) and PPARbeta activity. Biochemistry 42, 10726–10735.

Sumanasekera, W.K., Tien, E.S., Turpey, R., Vanden Heuvel, J.P., and Perdew, G.H. (2003b). Evidence that peroxisome proliferator-activated receptor alpha is complexed with the 90-kDa heat shock protein and the hepatitis virus B X-associated protein 2. J. Biol. Chem. 278, 4467–4473.

Turk, J., Wolf, B.A., Lefkowith, J.B., Stump, W.T., and McDaniel, M.L. (1986). Glucose-induced phopholipid hydrolysis in isolated pancreatic islets. Quantitative effects on the content of arachidonate and other fatty acids. Biochim. Biophys. Acta 879, 399–409.

Ullman, A.H., and White, H.B., III. (1981). Assay of fatty acid synthase using a bicyclic dione as substrate. Methods Enzymol. 72, 303–306.

Wisely, G.B., Miller, A.B., Davis, R.G., Thornquest, A.D., Jr., Johnson, R., Spitzer, T., Sefler, A., Shearer, B., Moore, J.T., Willson, T.M., et al. (2002). Hepatocyte nuclear factor 4 is a transcription factor that constitutively binds fatty acids. Structure 10, 1225–1234.

Wolf, B.A., Pasquale, S.M., and Turk, J. (1991). Free fatty acid accumulation in secretagogue-stimulated pancreatic islets and effects of arachidonate on depolarization-induced insulin secretion. Biochemistry 30, 6372–6379.

Wolfrum, C., Borrmann, C.M., Borchers, T., and Spener, F. (2001). Fatty acids and hypolipidemic drugs regulate peroxisome proliferator-activated receptors alpha- and gamma-mediated gene expression via liver fatty acid binding protein: a signaling path to the nucleus. Proc. Natl. Acad. Sci. USA 98, 2323–2328.

Xu, H.E., Lambert, M.H., Montana, V.G., Parks, D.J., Blanchard, S.G., Brown, P.J., Sternbach, D.D., Lehmann, J.M., Wisely, G.B., Willson, T.M., et al. (1999). Molecular recognition of fatty acids by peroxisome proliferator-activated receptors. Mol. Cell 3, 397–403.

Xu, J., Cho, H., O'Malley, S., Park, J.H., and Clarke, S.D. (2002a). Dietary polyunsaturated fats regulate rat liver sterol regulatory element binding proteins-1 and -2 in three distinct stages and by different mechanisms. J. Nutr. 132, 3333–3339.

Xu, J., Xiao, G., Trujillo, C., Chang, V., Blanco, L., Joseph, S.B., Bassilian, S., Saad, M.F., Tontonoz, P., Lee, W.N., and Kurland, I.J. (2002b). Peroxisome proliferator-activated receptor alpha (PPARalpha) influences substrate utilization for hepatic glucose production. J. Biol. Chem. 277, 50237–50244.

Yamamoto, T., Shimano, H., Nakagawa, Y., Ide, T., Yahagi, N., Matsuzaka, T., Nakakuki, M., Takahashi, A., Suzuki, H., Sone, H., et al. (2004). SREBP-1 interacts with hepatocyte nuclear factor-4 alpha and interferes with PGC-1 recruitment to suppress hepatic gluconeogenic genes. J. Biol. Chem. 279, 12027–12035.

Yang, T., Espenshade, P.J., Wright, M.E., Yabe, D., Gong, Y., Aebersold, R., Goldstein, J.L., and Brown, M.S. (2002). Crucial step in cholesterol homeostasis: sterols promote binding of SCAP to INSIG-1, a membrane protein that facilitates retention of SREBPs in ER. Cell 110, 489–500.